

# On high-quality electron beam generated by breaking wake wave in near-critical density plasmas

P. Valenta<sup>1,2</sup>, O. Klímo<sup>1,2</sup>, S. V. Bulanov<sup>1,3</sup>, G. Korn<sup>1</sup>

<sup>1</sup> *ELI Beamlines, Institute of Physics, Czech Academy of Sciences, Prague, Czech Republic*

<sup>2</sup> *Czech Technical University in Prague, Faculty of Nuclear Sciences and Physical Engineering, Prague, Czech Republic*

<sup>3</sup> *Kansai Photon Science Institute, National Institutes for Quantum and Radiological Science and Technology, Kizugawa, Kyoto, Japan*

High-quality and stable sub-relativistic electron sources are of great demand for various applications in industry and material science [1, 2]. The electron sources in such regime have been previously produced by downscaling a laser-wakefield accelerator or using high-repetition rate laser-plasma accelerators [3, 4, 5].

Here we describe a method based on the breaking of non-linear Langmuir waves driven by a short intense laser pulse in the near-critical density plasmas. We observe a formation of a thin layer of electrons that are expelled from the target at the plasma-vacuum interface. High quality of the electron bunch is provided using a steep density profile on the target rear side and proper parameters of the laser pulse. The electron beam has peak energy of several MeV, relatively high electric charge, and low divergence. We demonstrate this effect numerically using 2D large-scale particle-in-cell (PIC) simulations and provide analytical formulas that describe the properties of the electron bunch.

The PIC simulations have been performed using massively parallel plasma simulation code EPOCH [6]. A Gaussian linearly polarized laser pulse with the center wavelength  $\lambda = 1 \mu\text{m}$  propagates through narrow pre-ionized hydrogen plasma slab with the initial density profile prescribed by the following function,

$$n_{e,p}(x) = n_0 \exp \left[ \left( \frac{x - x_0}{d_0} \right)^{10} \right].$$

The maximum density  $n_0 = 0.05 n_c$  ( $\approx 5.6 \cdot 10^{19} \text{ cm}^{-3}$ ) is defined in terms of the critical density  $n_c = m_e \omega^2 / (4\pi e^2)$ , where  $m_e$  stands for the electron mass,  $e$  is the elementary charge and  $\omega = 2\pi c / \lambda$  is the angular frequency of the laser beam. The constant  $c$  denotes the velocity of light in vacuum. The density peak is located at  $x_0 = 12 \lambda$  and the parameter  $d_0 = 6 \lambda$ . The longitudinal line-out along the y-axis of the electron density can be seen in Fig. 1.

The laser parameters are chosen to be optimal for the excitation of the large-amplitude wake field [7]. The dimensionless amplitude of the laser beam  $a_0 \approx 2.5$  ( $I \approx 8.7 \cdot 10^{18} \text{ W} \cdot \text{cm}^{-2}$ ) is chosen such that the electric field in the generated wake waves stays below the Akhiezer-Polovin wave breaking limit [8]

$$E_{A-P} = \frac{m_e \omega_{pe} c}{e} \sqrt{2(\gamma_w - 1)},$$

where  $\omega_{pe} = \sqrt{4\pi n_e e^2 / m_e}$  is the electron plasma frequency and  $\gamma_w = 1 / \sqrt{1 - \beta_w^2}$  is defined in terms of  $\beta_w = v_{ph}/c$ . The phase velocity of the wake wave  $v_{ph}$  is equal to the group velocity of the laser beam  $v_g = c \sqrt{1 - \omega_{pe}^2 / \omega^2}$ .

The duration of the laser pulse  $\tau \approx 7.7$  fs in FWHM ( $\approx 2.3 T$ , where  $T = 2\pi/\omega$  is the laser period) is chosen such that the laser length corresponds to the half of the wake wave wavelength  $\lambda_w = \lambda \gamma_w E(-a_0^2) / \pi$ , where  $E(x)$  is the complete elliptic integral of the second kind [9].

The size of the simulation domain is  $60 \lambda$  in both directions, represented by approx.  $3.6 \cdot 10^7$  cells in total. The simulation setup corresponds to the resolution of 100 cells per  $\lambda$ , 16 additional cells are reserved for absorbing boundary conditions on each side of the simulation domain. The cell size is therefore  $\Delta x = \Delta y \approx 10 \text{ nm}$ . The simulation time-step is chosen to fulfill the CFL [10] condition  $\Delta t = C \Delta x / \sqrt{2}c$ , where the CFL number  $C = 0.95$ , therefore  $\Delta t \approx 22 \text{ as}$ . The simulation time is chosen to  $70 T$ , thus the whole simulation requires approximately  $1.0 \cdot 10^4$  iterations.

The plasma is cold throughout the target, which is initially at rest and is made of electrons and protons that are represented by weighted macro-particles. The number of particles per one simulation cell is 16 for both, electrons and protons. The protons are set to be immobile. The boundary conditions for particles are thermalizing. In total, the simulation domain contains approximately  $3.4 \cdot 10^8$  macro-particles.

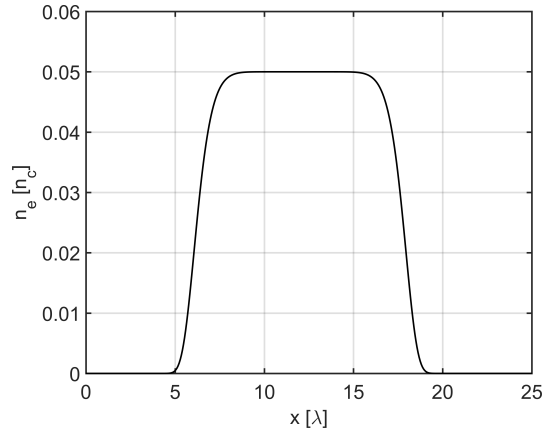


Figure 1: Longitudinal line-out along the y-axis of the electron density profile

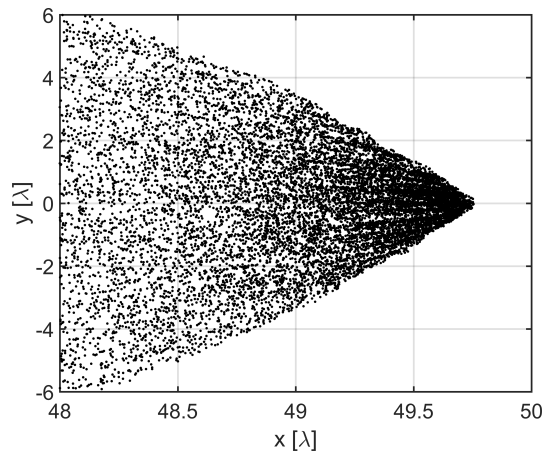


Figure 2: Electron density distribution in the bunch

The laser beam excites a strongly nonlinear Langmuir wave which propagates through plasma with the phase velocity equal to the group velocity of the laser beam and subsequently breaks due to the steep density drop at the rear side of the target. The part of the electrons contained in the plasma wave, whose kinetic energy is sufficient to overcome the electrostatic potential generated due to the electric charge separation, is expelled into vacuum forming a thin layer. Later on, this layer is transformed into the characteristic arrow-like shape since the electrons located in the vicinity of axis have slightly higher energy than the electrons at periphery (Fig. 2). As can be seen in the Fig. 3 the electrons are further accelerated after they exit the plasma due to the directed Coulomb explosion [11].

The properties of the accelerated electron bunch were collected and analyzed 40  $\mu\text{m}$  beyond the target rear side. The energy spectrum of the electrons in the bunch is relatively broad with the peak energy of 5 MeV (Fig. 3, Fig. 4). The number of electrons in the bunch predicted by simulations is in the range of  $5 \cdot 10^8 - 1 \cdot 10^9$ , therefore the electric charge is 100 – 150 pC. The duration of the bunch is lower than 10 fs and the divergence of the electrons varies from 30 mrad for the most energetic electrons at the front of the bunch to 60 mrad for the electrons in the low-energy tail (Fig. 5).

Let us find analytically the energy spectrum of electrons in the wake wave at the threshold of breaking in the one-dimensional approximation. The properties of the non-linear waves near singularities have been extensively studied [12]. Assume all functions to be dependent on the variable  $X = x - v_{ph}t$ , where  $x$  and  $t$  denote the space and

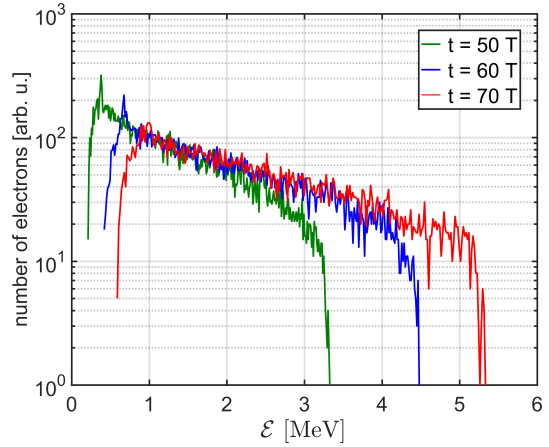


Figure 3: Energy spectra of the electron bunch at several different time instants

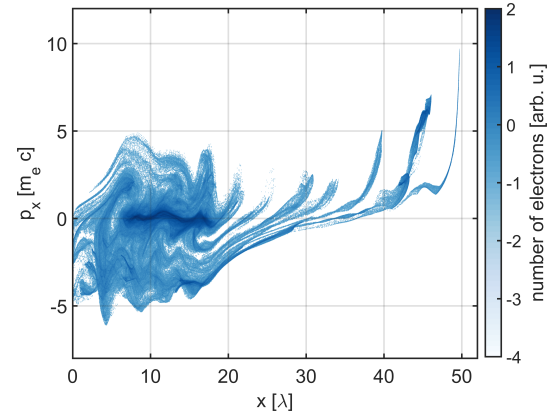


Figure 4: phase space ( $x$  vs.  $p_x$ ) of the electrons located in the vicinity of the axis  $y = 0$

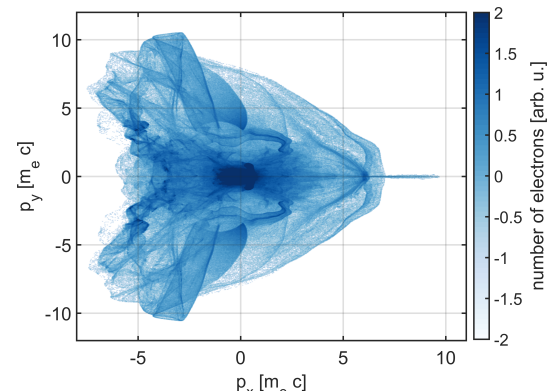


Figure 5: phase space ( $p_x$  vs.  $p_y$ ) of all the electrons in the simulation domain

time coordinate, respectively, and  $v_{ph}$  is the phase velocity of the wake wave. Consider the electron density in the wave to be  $n(X) \approx |X|^{-2/3}$  and the momentum of the electrons in the wave to be  $p(X) \approx p_m - |X|^{2/3}$ , where  $p_m = p(X_m)$  is the momentum at the wave-breaking coordinate  $X_m$ . The distribution function is then  $f(X, p) = |X|^{-2/3} \delta(p - p_m + |X|^{2/3})$ . Consequently, one can easily obtain the energy spectrum of the electrons,

$$\frac{dN}{dp} = \int_{-\infty}^{\infty} f(X, p) dX \approx \frac{1}{\sqrt{p_m - p}}.$$

In conclusion, we have studied the properties of the electron bunch generated by the breaking wake wave at the plasma-vacuum interface of narrow underdense targets. We have analytically estimated the energy spectrum of the bunch and performed several 2D PIC simulations to demonstrate this effect numerically. The simulations predict relatively high electric charge of the bunch and low divergence. Such beam can be further studied as a relativistic flying mirror [12], in terms of injection to the secondary wake field and various other applications such as ultrafast imaging [13] or femtosecond X-ray generation [14].

**Acknowledgement:** This work was supported by the project High Field Initiative (CZ.02.1.01 /0.0/0.0/15 003/0000449) from the European Regional Development Fund. Computational resources were provided by the ECLIPSE cluster of the ELI Beamlines. The development of the EPOCH code was funded in part by the UK EPSRC grants EP/G054950/1, EP/G056803/1, EP/G055165/1 and EP/M022463/1.

## References

- [1] G. Sciaiani and R.J.D. Miller, *Rep. Prog. Phys.* **74**, 096101 (2011)
- [2] Z.-H. He et al., *Sci. Rep.* **6**, 36224 (2016)
- [3] B. Beaurepaire, A. Lifschitz and J. Faure, *New Journal of Physics* **16**, 2 (2014)
- [4] D. Guenot et al., *Nature Photonics* **11**, 293–296 (2017)
- [5] D. Gustas et al., *Phys. Rev. Accel. Beams* **21**, 1 (2018)
- [6] T. D. Arber et al., *Plasma Phys. Control. Fusion* **57**, 11 (2015)
- [7] S. V. Bulanov et al., *J. Plasma Phys.* **82**, 05820308 (2016)
- [8] A. I. Akhiezer, R. V. Polovin, *Sov. Phys. JETP* **3**, 5 (1956)
- [9] S. Gradshteyn, I. M. Ryzhik, *Table of Integrals. Series, and Products*, Academic (1980)
- [10] R. Courant, K. Friedrichs, H. Lewy, *Mathematische Annalen* (in German), **100**, 1 (1928)
- [11] S. S. Bulanov et al., *Phys. Rev. E* **78**, 026412 (2008)
- [12] S. V. Bulanov et al., *Physics - Uspekhi* **56**, 429 (2013)
- [13] R. J. D. Miller, *Science* **343**, 6175 (2014)
- [14] S. Corde, et al. *Rev. Mod. Phys.* **85**, 1 (2013)